ISSN(O): 2320-9801
ISSN(P): 2320-9798


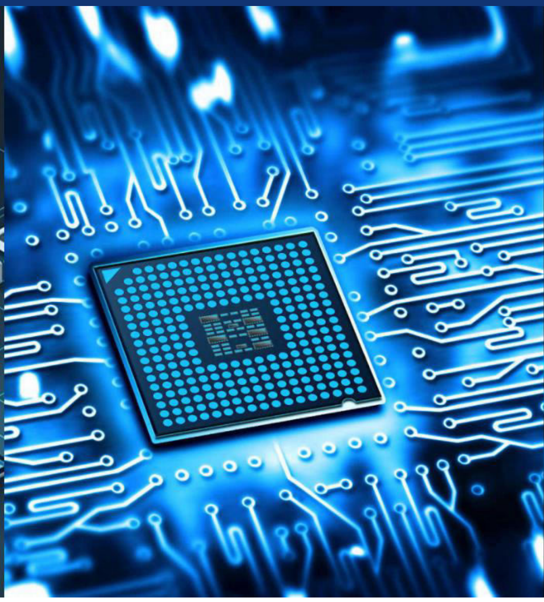


International Journal of Innovative Research in Computer and Communication Engineering

(A Monthly, Peer Reviewed, Refereed, Scholarly Indexed, Open Access Journal)

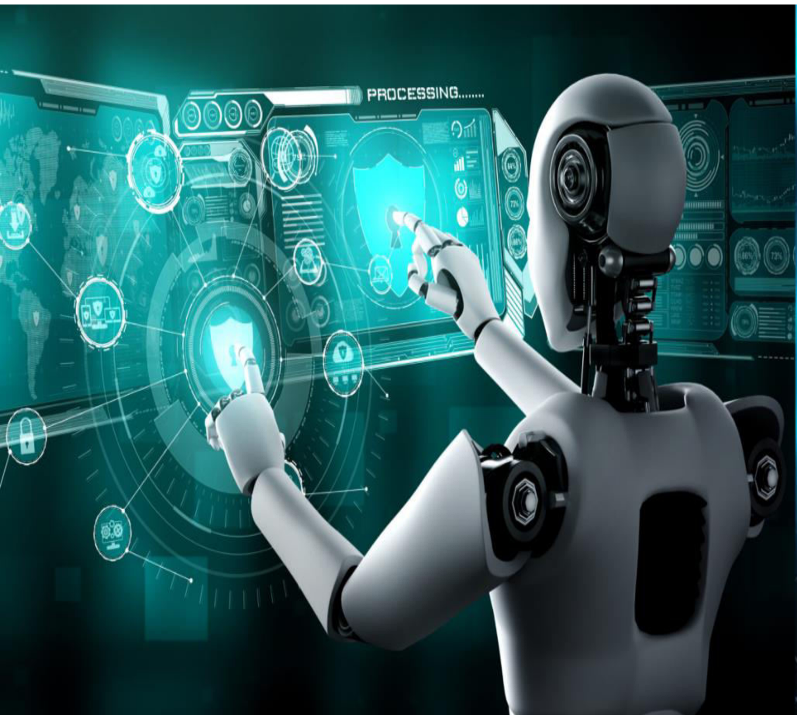

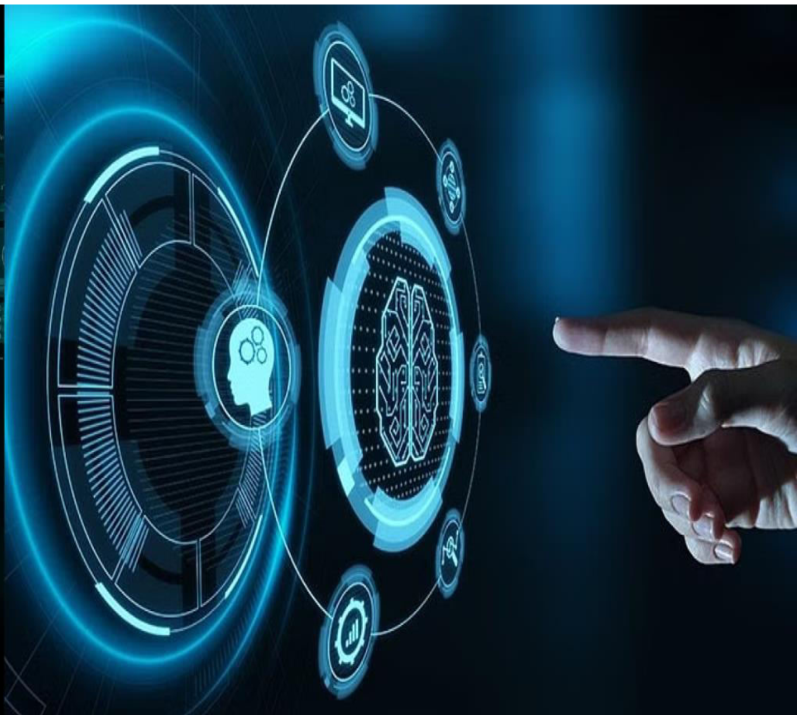

Impact Factor: 9.927

Volume 14, Issue 7, July 2026

© 2026 IJIRCCE | Volume 14, Issue 7, July 2026 DOI: 10.15680/IJIRCCE.2026.1407071

www.ijircce.com | e-ISSN: 2320-9801, p-ISSN: 2320-9798| Impact Factor: 9.927| ESTD Year: 2013|

International Journal of Innovative Research in Computer and Communication Engineering (IJIRCCE)

(A Monthly, Peer Reviewed, Refereed, Scholarly Indexed, Open Access Journal)

Brain Tumour Classification: Methods, Technologies and a Comparative Review

Dr Gururaj J.P

Associate Professor, Government First Grade College, Davangere, India

ABSTRACT: One of the most dangerous neurological conditions is brain tumours, and patient survival and treatment planning are directly impacted by early and accurate diagnosis. The main non-invasive method for visualizing tumours is still magnetic resonance imaging (MRI), and computer-aided diagnosis (CAD) systems based on deep learning and machine learning have gradually automated the classification of meningioma, glioma, pituitary, and other tumour types. The main paradigms for brain tumour classification are compared in this review in an organized, mathematically grounded manner: (i) deep Convolutional Neural Networks (CNNs) and transfer-learning architectures such as VGG16/19, ResNet50, InceptionV3, Xception, DenseNet, MobileNet, and EfficientNet; (ii) classical machine learning pipelines that rely on handcrafted texture and statistical features such as the Gray-Level Co-occurrence Matrix (GLCM), Discrete Wavelet Transform (DWT), and Principal Component Analysis (PCA). (g). ResViT, UNetFormer, TECNN); and (iv) ensemble and hybrid approaches that combine learned and manually created features. The underlying mathematical formulation for each family of methods is derived and explained, and performance figures from recent literature are tabulated on widely used benchmark datasets (Figshare CE-MRI, BraTS, Kaggle Brain Tumour MRI Dataset, Br35H, and SARTAJ). A comparison of accuracy-complexity trade-offs, an overview of unresolved issues, and future directions like multimodal fusion, explainable AI, and quantum machine learning round out the review.

KEYWORDS: Brain tumour classification, MRI, Convolutional Neural Networks, transfer learning, Vision Transformer, GLCM, SVM, deep learning, computer-aided diagnosis.

I. INTRODUCTION

One of the most serious and potentially fatal neurological conditions are brain **tumour**s, which are caused by aberrant and unchecked cell growth in the brain or surrounding tissues. Brain tumours can be categorized as primary or secondary (metastatic), benign or malignant, based on their biological features and place of origin. Gliomas, meningiomas, pituitary tumours, and metastatic tumours are common types of brain tumours; each has unique pathological characteristics and treatment needs. Global cancer statistics show that brain and central nervous system tumours have a major impact on long-term neurological disability and cancer-related mortality. Therefore, effective treatment planning, surgical intervention, radiotherapy, chemotherapy, and increased patient survival depend on an early and accurate diagnosis. Because of its superior soft-tissue contrast, high spatial resolution, and non-invasive imaging capability, magnetic resonance imaging (MRI) has emerged as the favored imaging modality for brain tumour diagnosis.

A variety of MRI sequences, such as T1-weighted, T2-weighted, Fluid-Attenuated Inversion Recovery (FLAIR), and contrast-enhanced T1 (T1CE), offer complementary anatomical and pathological information that helps medical professionals recognize the boundaries of tumours, edema, necrotic areas, and surrounding healthy tissues. However, manually interpreting MRI scans is a laborious procedure that is susceptible to inter-observer variability and heavily relies on radiologists' experience. The need for automated computer-aided diagnosis (CAD) systems that can assist physicians by offering quick, accurate, and consistent tumour classification has been further highlighted by the rise in medical imaging tests.

The classification of brain tumours has advanced significantly over the last 20 years thanks to developments in deep learning, machine learning, and artificial intelligence. Gray-Level Co-occurrence Matrix (GLCM), Local Binary Patterns (LBP), Histogram of Oriented Gradients (HOG), Discrete Wavelet Transform (DWT), and Principal Component Analysis (PCA) were among the manually developed feature extraction techniques that were the mainstay of early computer-aided diagnosis systems. Traditional machine learning algorithms like Support Vector Machines

www.ijircce.com | e-ISSN: 2320-9801, p-ISSN: 2320-9798| Impact Factor: 9.927| ESTD Year: 2013|

International Journal of Innovative Research in Computer and Communication Engineering (IJIRCCE)

(A Monthly, Peer Reviewed, Refereed, Scholarly Indexed, Open Access Journal)

(SVM), k-Nearest Neighbors (KNN), Random Forest (RF), Decision Trees, Naïve Bayes, and Artificial Neural Networks (ANN) were then used to classify these manually created features. Despite showing encouraging results on comparatively small datasets, these methods' reliance on manually created feature engineering hindered their capacity to generalize across various imaging conditions and tumour variations. By enabling automatic hierarchical feature learning from raw MRI images, deep learning has completely changed medical image analysis.

Due to their capacity to learn discriminative spatial representations without the need for manual feature extraction, Convolutional Neural Networks (CNNs) have emerged as the predominant framework for brain tumour classification. AlexNet, VGG16, VGG19, ResNet, DenseNet, InceptionV3, Xception, MobileNet, EfficientNet, and ConvNeXt are just a few of the transfer learning architectures that have been effectively modified for MRI-based tumour classification, yielding notable gains in robustness and accuracy. By simulating long-range spatial relationships within medical images, attention mechanisms and Vision Transformer (ViT) architectures have more recently improved classification performance. Hybrid models that combine CNNs with Transformer networks, explainable artificial intelligence (XAI) techniques, and ensemble learning strategies have shown state-of-the-art outcomes while enhancing clinical confidence and model interpretability.

The extensive clinical use of automated brain tumour classification systems is still constrained by a number of issues, despite these noteworthy developments. Compared to natural image datasets, publicly accessible MRI datasets are still quite small, which results in overfitting and poor model generalization. Cross-institutional performance is negatively impacted by significant domain shifts brought about by differences in imaging protocols, scanner manufacturers, acquisition parameters, and patient demographics. Adoption of deep learning models in routine clinical practice is further complicated by class imbalance, noisy annotations, computational complexity, and the "black-box" nature of these models. Furthermore, research on ensuring robustness, fairness, interpretability, and regulatory compliance of dependable models is still ongoing. Inspired by these difficulties, this review provides a thorough overview of the techniques and tools utilized for MRI-based brain tumour classification.

The entire classification pipeline—image acquisition, preprocessing, segmentation, handcrafted feature extraction, deep learning architectures, transfer learning models, attention mechanisms, Vision Transformers, hybrid learning approaches, and explainable AI techniques—is methodically examined in this paper. In order to gain theoretical understanding of the learning mechanisms of popular algorithms, their mathematical underpinnings are examined. In order to highlight the advantages and disadvantages of current methods, the review also contrasts benchmark datasets, performance evaluation metrics, computational complexity, and published classification results from recent literature. This review offers a unified comparison of conventional machine learning, deep learning, transformer-based architectures, and hybrid models within a common analytical framework, in contrast to many other surveys that concentrate on a single category of techniques. Multimodal learning, federated learning, self-supervised learning, lightweight neural networks, explainable artificial intelligence, and foundation models for medical image analysis are just a few of the research gaps, emerging technologies, and future research opportunities that are covered. This review attempts to be a thorough resource for researchers, clinicians, and practitioners working toward precise, effective, and reliable brain tumour classification systems by combining methodological comparisons, mathematical analysis, performance evaluation, and future perspectives.

II. LITERATURE REVIEW

The research trajectory of automated brain tumour classification from MRI images is reviewed in this section. It starts the deep learning transformation (2016–2021), and ends with the current era of transfer learning, attention mechanisms, and hybrid CNN-Transformer models (2022–2026). Following a thematic synthesis that highlights recurrent design decisions and enduring gaps that inspire the mathematical and comparative analysis presented in the rest of this paper, studies are arranged chronologically within each era and summarized in terms of methodology, dataset, and reported performance.

2.1 Era II — Deep Learning and the CNN Transition (2016-2021)

Brain tumour classification in the mid-to-late 2010s was dominated by Convolutional Neural Networks, trained from scratch but increasingly via transfer learning from ImageNet-pretrained backbones, mirroring the rising availability of the Figshare CE-MRI dataset (Cheng et al., 2015) and the BraTS benchmark.

www.ijircce.com | e-ISSN: 2320-9801, p-ISSN: 2320-9798| Impact Factor: 9.927| ESTD Year: 2013|

International Journal of Innovative Research in Computer and Communication Engineering (IJIRCCE)

(A Monthly, Peer Reviewed, Refereed, Scholarly Indexed, Open Access Journal)

Paul et al. Using the Figshare dataset directly for three-class tumour classification, Tsang et al.(2017) were some of the first to demonstrate that CNNs are applicable to this problem without using handcrafted features. The widely cited transfer-learning study applied architectures of AlexNet, GoogLeNet, and VGG on the Figshare dataset with a maximum accuracy of 98.69% observed for VGG16. Khan et al. In this direction, Jiang et al. (2020) used transfer learning from a VGG16 model on the BraTS dataset, achieving an accuracy of 96.27% and successfully demonstrating that even across the more complex, multi-institution datasets such as BraTS transfer learning can be useful. For instance, Çinar and Yildirim (2020) suggested a variant of ResNet50 architecture that uses an expanded, dilation-augmented region only in the primary tumour area to deliver localized predictions. Sultan et al. They proposed a CNN architecture validated both in the Figshare dataset and on a separate, locally acquired T1-weighted dataset exploring cross-dataset evaluation, a topic that was still uncommon at the time (2019).

This era also saw the emergence of hybrid sequence aware architectures in 2019 study integrated a pretrained AlexNet backbone with simple pruned one-dimensional DWT-based feature compression and an LSTM classifier to perform liver and brain lesion classification, showing early investigations into CNN-recurrent hybrids. Transfer-learning CNNs (which were performing best, also in generalization performance on the multi-class tasks) had become the most common approach by this time, although the majority of studies still used single full-dataset train/test splits from the Figshare dataset without cross-validation or external testing.

2.2 Era III — Transfer Learning Maturity, Optimization, and Explainability (2022-2024)

This time was marked by the first systematic large scale comparison between pre-trained CNN backbones, inclusion of meta-heuristic optimization methods and serious action to interpret models.

Maqsood et al. (2022) systematically evaluated VGG16, VGG19, ResNet50 and DenseNet21 when trained with four optimizers (Adadelta, Adam, RMSprop SGD) on the Figshare dataset and reported that amongst all compared backbones, VGG16 optimized with Adadelta performed best with a accuracy of 99.02%. Kaplan et al. applied nLBP and αLBP local binary pattern feature-extraction variants with a KNN classifier reaching 95.56% accuracy, signaling continued interest in hybrid handcrafted-plus-classical-ML pipelines even as CNNs came-of-age. Sharma et al. (2023) compared a custom CNN, VGG and ResNet50 on a four-class dataset derived from Kaggle and reported ~95% accuracy but used one random split with no cross-validation, ablation or interpretability analysis methodologically limiting results for other studies that specifically set out to address. A 2023 study combining Xception, ResNet50, InceptionV3, VGG16 and MobileNet on the Figshare dataset were reported with an F1-score of 98.75%, 98.50%, 98.00%, 97.50% and 97.25% respectively for a more thorough five-architecture comparison available during this period

Abdusalomov et al. (2024) implemented YOLOv7 and transfer learning achieving 99.5% accuracy on common tumour types, extending the use of object-detection architectures to this classification task. Mohamed Mustafa et al. (2024) adapted ResNet50 to use as-modified Grad-CAM for binary tumour classification of an esophageal cancer dataset from Kaggle, reporting 98.52% accuracy while directly integrating qualitative saliency-map interpretability — part of a growing trend toward explainable modeling pipelines employing supervised methods with interpretive nature such as Grad-CAM, Grad-CAM++ and LIME. An Similarly 2024 study fused GAN-based data augmentation with ResNet50 and LIME explainability reports a accuracy score of 99.53%. Additionally, in this period an attention-augmented GoogLeNet-style CNN was developed for computationally efficient classification, and a hybrid EfficientNetB0 plus a new quantum genetic algorithm are described, representing early research on metaheuristic and quantum-inspired optimization approaches .

2.3 Era IV — Attention, Vision Transformers, and Rigor-Focused Evaluation (2025-2026)

Recent literature is characterized by two concurrent trends: the adoption of attention mechanisms and Vision Transformers for modeling global context, combined with an increased emphasis on rigorous, cross-validated, interpretable evaluation protocols in light of methodological concerns highlighted in earlier work.

Han et al. (2025) and revealed in-depth prescriptive lessons on the image regions to attend to based on backbone (VGG16, ResNet50, and EfficientNet) at prediction time — an important finding for clinical trust although this study's main focus was a relative architecture comparison instead of establishing a rigorously validated single-model baseline using either LIME or Grad-CAM. It was in this context that a study from 2026 first presented a fully cross-validated ResNet50 model without structural priors, with fine-tuning and ablation of regularization and augmentation, reporting

www.ijircce.com | e-ISSN: 2320-9801, p-ISSN: 2320-9798| Impact Factor: 9.927| ESTD Year: 2013|

International Journal of Innovative Research in Computer and Communication Engineering (IJIRCCE)

(A Monthly, Peer Reviewed, Refereed, Scholarly Indexed, Open Access Journal)

an accuracy of 96.67% (macro-F1 =0.9658) after structured analysis of Grad-CAM++ failure modes on no-tumour slices. In 2025, a study achived solid multi-class perforamnce on the combined (7,023-image) Figshare/SARTAJ/Br35H while also explicitly analzying convergence stability through fin-tuning ResNet34 with a custom classification head and using the Ranger optimizer (a combination of RAdam and Lookahead).

At the architecture level, systematic reviews of 2022-2025 show incremental inclusion of Vision Transformers (ViT), three-dimensional ViT3D models and hybrid CNN-Transformer architectures like ResViT, UNetFormer and TECNN with attention and global context used in conjunction with convolutions local feature extraction. It is shown in a comparative analysis to 2025 resource efficient container neural network architectures, that less complex and better designed custom neural networks (98.67% − 99.62 on binary tasks, 98.09 on multi-class task) trained from scratch can do just as good/better at using substantially less computational cost over more deeper pretrained containers such as ResNet18 and VGG16 with additional testing performed under data-efficiency conditions (0 − 80 shots for few-shot learning). In a separate development, variational quantum classifiers have also been studied in an exploratory setting for benchmarking brain tumour MRI classification models as potential candidates to provide robustness and explainability relative to established classical deep learning baselines (though this field is still at a proof-of-concept stage).

2.4 Chronological Summary Table

Year	Study / Authors	Method	Dataset	Reported Result	Key Limitation
2017	Paul et al.	CNN (from scratch)	Figshare CE-MRI	Competitive 3-class accuracy	No transfer learning; single split
2019	AlexNet/GoogLeNet/VGG TL study	Transfer learning (VGG16 best)	Figshare CE-MRI	98.69% accuracy	Limited cross-validation
2020	Khan et al.	Fine-tuned VGG16	BraTS	96.27% accuracy	BraTS heterogeneity lowers accuracy
2020	Çinar & Yildirim	Modified ResNet50 + ROI augmentation	Figshare CE-MRI	Improved localization-aware accuracy	Added preprocessing complexity
2022	Maqsood et al.	VGG16/19, ResNet50, DenseNet21 (4 optimizers)	Figshare CE-MRI	99.02% (ResNet50 + Adadelta)	Single-source dataset
2022	Kaplan et al.	nLBP / αLBP features + KNN	MRI (multi-type)	95.56% accuracy	Limited scalability of handcrafted features
2023	Sharma et al.	Custom CNN, VGG, ResNet50	Kaggle (4-class)	~95% accuracy	Single split, no cross-validation or XAI
2023	5-model TL comparison	Xception/ResNet/Inception/VGG/MobileNet	Figshare CE-MRI	F1: 97.25%-98.75%	No attention/Transformer comparison
2024	Abdusalomov	YOLOv7 + transfer learning	MRI (common	99.5%	Detection-oriented

www.ijircce.com | e-ISSN: 2320-9801, p-ISSN: 2320-9798| Impact Factor: 9.927| ESTD Year: 2013|

International Journal of Innovative Research in Computer and Communication Engineering (IJIRCCE)

(A Monthly, Peer Reviewed, Refereed, Scholarly Indexed, Open Access Journal)

Year	Study / Authors	Method	Dataset	Reported Result	Key Limitation
	et al.		types)	accuracy	framing
2024	Mohamed Mustafa et al.	ResNet50 + Grad-CAM	Kaggle-derived	98.52% accuracy (binary)	Binary labels; qualitative XAI only
2024	GAN + ResNet50 + LIME study	GAN augmentation + ResNet50 + LIME	Kaggle-type dataset	99.53% accuracy	Risk of GAN-induced synthetic bias
2025	Han et al.	VGG16/ResNet50/EfficientNet + LIME/Grad-CAM	MRI (multi-class)	Backbone-dependent attended regions	Comparative focus, not a validated baseline
2025	ResNet34 + Ranger optimizer study	Fine-tuned ResNet34, custom head	Figshare+SARTAJ+Br35H (7,023 img)	Strong 4-class performance	SARTAJ label noise in aggregated set
2025	Resource-efficient CNN comparison	Custom CNN vs. ResNet18/VGG16, few-shot	Br35H, Kaggle MRI Dataset	98.09%-99.62% accuracy	Gains may not transfer across scanners
2026	Fine-tuned ResNet50 (5-fold CV study)	ResNet50 + ablation + Grad-CAM++	Kaggle-derived (4-class)	96.67% acc., macro-F1 0.9658	Lower accuracy but more rigorous validation
2026	Variational Quantum Classifier study	Quantum ML (VQC) benchmark	Standard brain MRI sets	Exploratory / proof-of-concept	Not yet competitive at scale

III. PRE-PROCESSING TECHNIQUES

Pre-processing improves signal quality and reduces inter-scan variability before feature extraction or network training. Standard operations include:

- Denoising — median filtering or Gaussian high-pass filtering to suppress acquisition noise.
- Skull stripping — removal of non-brain tissue using morphological operations or atlas-based masks.
- Intensity normalization — rescaling pixel intensities, typically to [0, 1] or zero-mean/unit-variance, to stabilize gradient-based training.
- Bias-field correction — correcting low-frequency intensity inhomogeneity common in MRI (e.g., N4 bias correction).
- Data augmentation — rotation, flipping, scaling, and GAN-based synthetic sample generation to counter the limited size of medical imaging datasets and class imbalance.

Min–max intensity normalization is defined as:

$$I\_norm(x,y) = [I(x,y) - I\_min] / [I\_max - I\_min] \qquad (1)$$

where I(x,y) is the raw pixel intensity at location (x,y), and I_min, I_max are the minimum and maximum intensities in the image.

www.ijircce.com | e-ISSN: 2320-9801, p-ISSN: 2320-9798| Impact Factor: 9.927| ESTD Year: 2013|

International Journal of Innovative Research in Computer and Communication Engineering (IJIRCCE)

(A Monthly, Peer Reviewed, Refereed, Scholarly Indexed, Open Access Journal)

IV. HANDCRAFTED FEATURE EXTRACTION AND MATHEMATICAL FORMULATION

Traditional pipelines depend on descriptors that quantify texture, intensity distribution, or frequency content of the tumour region. The three most common families are GLCM, Discrete Wavelet Transform, and PCA.

4.1 Gray-Level Co-occurrence Matrix (GLCM)

GLCM captures second-order texture statistics by tabulating how frequently pairs of pixel intensities i and j occur at a specified spatial offset (Δx, Δy). Let P(i, j) denote the normalized co-occurrence probability. Key GLCM-derived features used in brain tumour classification include:

$\text{Contrast} = \Sigma_i \Sigma_j (i - j)^2 \cdot P(i, j)$ (2)

$\text{Energy} = \Sigma_i \Sigma_j [P(i, j)]^2$ (3)

$\text{Homogeneity} = \Sigma_i \Sigma_j P(i, j) / [1 + (i - j)^2]$ (4)

$\text{Correlation} = \Sigma_i \Sigma_j (i - \mu_i)(j - \mu_j) P(i, j) / (\sigma_i \sigma_j)$ (5)

Additional statistics — entropy, sum-mean, and variance — are frequently aggregated to form a feature vector of 8–20 dimensions per ROI, which is then passed to a classical classifier such as SVM or KNN.

4.2 Discrete Wavelet Transform (DWT)

DWT decomposes an image into approximation and detail sub-bands across multiple resolution levels, capturing both spatial and frequency information. For a 2-D image, one level of decomposition is expressed as:

$W_\varphi(j_0, m, n) = (1/\sqrt{MN}) \Sigma_x \Sigma_y I(x,y) \varphi_{j_0,m,n}(x,y)$ (6)

$W_\psi^i(j, m, n) = (1/\sqrt{MN}) \Sigma_x \Sigma_y I(x,y) \psi^i_{j,m,n}(x,y), \; i = \{H, V, D\}$ (7)

where φ is the scaling (approximation) function, ψ^i are the horizontal, vertical, and diagonal wavelet (detail) functions, and j_0 is the starting scale. Wavelet energy and wavelet entropy computed from the resulting sub-bands are widely used as compact, noise-robust texture descriptors, often combined with KNN or Naive Bayes classifiers.

4.3 Principal Component Analysis (PCA) for Dimensionality Reduction

Given a feature matrix $X \in \mathbb{R}^{n\times d}$ of n samples and d handcrafted features, PCA projects the data onto the eigenvectors of the covariance matrix that capture maximal variance:

$\Sigma = (1/n) \Sigma_i (x_i - \bar{x})(x_i - \bar{x})^T$ (8)

$\Sigma v_k = \lambda_k v_k$ (9)

The top-k eigenvectors $\{v_1,\ldots,v_k\}$ (ranked by eigenvalue λ_k) form the projection matrix used to reduce feature dimensionality before classification, mitigating the curse of dimensionality and reducing computational cost, at the potential loss of some discriminative information.

V. TRADITIONAL MACHINE LEARNING CLASSIFIERS

Once handcrafted features are extracted, a discriminative classifier maps the feature vector to a tumour class label. The four classifiers most reported in the literature are:

5.1 Support Vector Machine (SVM)

SVM seeks the maximum-margin hyperplane separating classes in feature space. For a linearly separable binary problem with training pairs (x_i, y_i), $y_i \in \{-1, +1\}$, the optimization is:

$\min_{w,b} \; \frac{1}{2}\|w\|^2 \;$ subject to $\; y_i(w^T x_i + b) \geq 1, \; \forall i$ (10)

For non-linearly separable data, a soft-margin formulation introduces slack variables ξ_i and a penalty parameter C:

$\min_{w,b,\xi} \; \frac{1}{2}\|w\|^2 + C \Sigma_i \xi_i \;$ subject to $\; y_i(w^T x_i + b) \geq 1 - \xi_i, \; \xi_i \geq 0$ (11)

Non-linear class boundaries are handled via the kernel trick, most commonly the Radial Basis Function (RBF) kernel:

$K(x_i, x_j) = \exp(-\gamma \|x_i - x_j\|^2)$ (12)

SVM with RBF or polynomial kernels applied to GLCM/DWT feature vectors has repeatedly reported accuracies above 95–99% on the Figshare and BraTS-derived binary (tumour vs. no-tumour) tasks, though performance degrades on multi-class, multi-institution data.

5.2 k-Nearest Neighbors (KNN)

KNN is a non-parametric, instance-based classifier that assigns a test sample the majority label among its k nearest neighbors in feature space, typically using Euclidean distance:

$d(x, x_i) = \sqrt{\Sigma_j (x_j - x_{ij})^2}$ (13)

www.ijircce.com | e-ISSN: 2320-9801, p-ISSN: 2320-9798| Impact Factor: 9.927| ESTD Year: 2013|

International Journal of Innovative Research in Computer and Communication Engineering (IJIRCCE)

(A Monthly, Peer Reviewed, Refereed, Scholarly Indexed, Open Access Journal)

KNN combined with wavelet-energy or LBP features is computationally inexpensive and has achieved reported accuracies in the 92–96% range for tumour-type classification, but its performance is sensitive to the choice of k and to feature scaling.

5.3 Random Forest and Decision Trees

Random Forest is an ensemble of decision trees trained on bootstrap-sampled subsets of the data and random feature subsets, with the final prediction obtained by majority voting. Node splits in each tree minimize impurity, commonly measured via the Gini index:

$$\mathrm{Gini}(t) = 1 - \Sigma_c [p(c|t)]^2 \qquad (14)$$

where $p(c|t)$ is the proportion of class c samples at node t. Hybrid ensemble classifiers combining KNN, Random Forest, and Decision Trees via majority voting have been reported to improve robustness over any single classical classifier while retaining low computational cost relative to deep networks.

5.4 Naive Bayes

Naive Bayes applies Bayes' theorem under a conditional-independence assumption between features:

$$P(c \mid x) = [P(x \mid c) \cdot P(c)] / P(x) \propto P(c)\, \Pi_j\, P(x_j \mid c) \qquad (15)$$

It is computationally lightweight and often used as a baseline in wavelet-entropy-based classification pipelines, typically trailing SVM and ensemble methods in reported accuracy.

VI. DEEP LEARNING: CONVOLUTIONAL NEURAL NETWORKS

CNNs replace handcrafted feature engineering with learned hierarchical representations, and since roughly 2018 have become the dominant approach to brain tumour classification. A CNN alternates convolutional, non-linear activation, and pooling layers before a fully connected classification head.

6.1 Convolution and Pooling Operations

The 2-D discrete convolution of an input feature map I with a learnable kernel K of size (2a+1)×(2b+1) is:

$$S(i, j) = (I * K)(i, j) = \Sigma_m \Sigma_n I(i - m, j - n)\, K(m, n) \qquad (16)$$

A bias term and non-linear activation — most commonly the Rectified Linear Unit (ReLU) — are then applied element-wise:

$$f(z) = \max(0, z) \qquad (17)$$

Max-pooling performs spatial down-sampling and provides translation invariance by retaining the maximum activation in each local window R:

$$P(i, j) = \max_{(m,n) \in R(i,j)} S(m, n) \qquad (18)$$

The final fully connected layer maps the flattened feature vector to class scores via the softmax function, producing a probability distribution over C tumour classes:

$$\hat{y}_c = \mathrm{softmax}(z)_c = e^{z_c} / \Sigma_{k=1}^{C} e^{z_k} \qquad (19)$$

Training minimizes the categorical cross-entropy loss between predicted probabilities $\hat{y}$ and one-hot ground-truth labels y over N training samples:

$$L = -(1/N)\, \Sigma_i \Sigma_c\, y_{i,c} \log(\hat{y}_{i,c}) \qquad (20)$$

Parameters are updated via backpropagation and stochastic gradient-based optimizers (SGD, Adam, RMSprop, or Adadelta), e.g. for Adam:

$$\theta_{t+1} = \theta_t - \eta \cdot \hat{m}_t / (\sqrt{\hat{v}_t} + \varepsilon) \qquad (21)$$

where $\hat{m}_t$ and $\hat{v}_t$ are bias-corrected first and second moment estimates of the gradient, η is the learning rate, and ε prevents division by zero.

6.2 Custom vs. Pre-trained CNNs

Studies broadly split into custom, relatively shallow CNNs designed specifically for brain MRI, which can be competitive and computationally efficient at 98–99.6% accuracy on binary and multi-class Figshare/Kaggle tasks while using far fewer parameters than deep pre-trained networks, and transfer-learning approaches that fine-tune networks pre-trained on ImageNet.

© 2026 IJIRCCE | Volume 14, Issue 7, July 2026 DOI: 10.15680/IJIRCCE.2026.1407071

www.ijircce.com | e-ISSN: 2320-9801, p-ISSN: 2320-9798| Impact Factor: 9.927| ESTD Year: 2013|

International Journal of Innovative Research in Computer and Communication Engineering (IJIRCCE)

(A Monthly, Peer Reviewed, Refereed, Scholarly Indexed, Open Access Journal)

VII. TRANSFER LEARNING

Transfer learning re-uses convolutional filters learned on large natural-image corpora (typically ImageNet) and fine-tunes the later layers, or the entire network at a reduced learning rate, on the (comparatively small) brain MRI dataset. This mitigates the data-scarcity problem inherent to medical imaging. The most frequently benchmarked architectures are summarized below.

Table 7. Representative transfer-learning CNN architectures used for brain tumour classification and reported accuracy ranges compiled from recent studies.

Architecture	Depth / Key Idea	Reported Accuracy Range	Typical Dataset
VGG16 / VGG19	16–19 layers; stacked 3×3 convolutions	96.3% – 99.1%	Figshare, Kaggle, BraTS
ResNet50 / ResNet34	Residual (skip) connections mitigate vanishing gradients	94.8% – 99.5%	Figshare, Kaggle
InceptionV3	Multi-scale parallel convolutional filters	95.0% – 98.3%	Figshare, Kaggle
Xception	Depthwise-separable convolutions	~98.75% (F1)	Figshare
DenseNet	Dense feature-reuse connections between layers	Mid-range, competitive with ResNet	Kaggle
MobileNet / MobileNetV2	Lightweight depthwise-separable convolutions for edge deployment	97.3% – 99.1%	Figshare
EfficientNet (B0–B4)	Compound scaling of depth/width/resolution	Top-tier, among best-performing families	Figshare, Kaggle

VIII. ATTENTION MECHANISMS AND VISION TRANSFORMERS

Since 2022–2023, attention mechanisms and Vision Transformers (ViT) have been introduced to brain tumour classification to model long-range spatial dependencies that convolutional receptive fields capture only indirectly.

8.1 Self-Attention

The scaled dot-product self-attention mechanism, the core operation of the Transformer, computes a weighted combination of value vectors V using similarity between query Q and key K projections:

$$\text{Attention}(Q, K, V) = \text{softmax}(QK^T / \sqrt{d\_k})\, V \qquad (22)$$

where d_k is the dimensionality of the key vectors, used as a scaling factor to stabilize gradients. Multi-head attention runs several such operations in parallel on learned projections of Q, K, V and concatenates the results, allowing the model to attend to different representation subspaces simultaneously.

8.2 Vision Transformer (ViT) and Hybrid CNN-Transformer Models

ViT partitions an image into fixed-size patches, linearly embeds them with positional encodings, and processes the resulting sequence through standard Transformer encoder blocks. Because pure ViTs are data-hungry, brain tumour classification research has favored hybrid designs that combine convolutional local feature extraction with Transformer-based global context modeling. Notable examples reported in the 2022–2025 literature include ViT3D (volumetric ViT for 3-D MRI), ResViT and UNetFormer (CNN-Transformer hybrids), MobileViT (lightweight hybrid for on-device inference), and attention-guided residual multiscale CNNs (e.g., ARM-Net) and attention-based GoogLeNet-style CNNs, which insert channel or spatial attention modules into convolutional backbones rather than adopting a full Transformer encoder.

www.ijircce.com | e-ISSN: 2320-9801, p-ISSN: 2320-9798| Impact Factor: 9.927| ESTD Year: 2013|

International Journal of Innovative Research in Computer and Communication Engineering (IJIRCCE)

(A Monthly, Peer Reviewed, Refereed, Scholarly Indexed, Open Access Journal)

These architectures generally report accuracy and F1-scores competitive with or exceeding the strongest pure-CNN transfer-learning baselines (often in the upper 90s percent range), with the additional benefit of attention maps that can support interpretability, at the cost of higher computational and memory requirements relative to lightweight CNNs such as MobileNet.

8.3. Hybrid and Ensemble Approaches

A substantial portion of recent work combines multiple methods rather than relying on a single classifier or architecture:

- CNN feature extraction + classical classifier: deep CNN or pre-trained backbone features are fed into an SVM or KNN classifier rather than a softmax layer, combining learned representations with the strong margin-based decision boundary of SVM.
- CNN + Recurrent/Sequential models: CNN–LSTM hybrids treat spatial CNN features as a sequence (e.g., across slices or wavelet sub-bands) to capture additional structure, sometimes combined with DWT-based feature strengthening prior to LSTM classification.
- Multi-model ensembling: parallel CNN branches (e.g., AlexNet + VGGNet) with feature-level fusion followed by a softmax classifier, or ensemble voting across independently trained backbones (Xception, ResNet50, InceptionV3, VGG16, MobileNet).
- Metaheuristic-optimized hybrids: architectures such as MobileNetV2 combined with optimization algorithms (e.g., Chaos Function Optimization) or genetic/quantum-genetic algorithms tuning hyperparameters of EfficientNet-based pipelines.
- Explainable hybrid pipelines: CNN backbones paired with Grad-CAM, Grad-CAM++, or LIME to visualize the image regions driving classification decisions, increasingly considered essential for clinical trust rather than optional.

Hybrid pipelines frequently report the highest published accuracies (often above 99%) but at the cost of increased architectural complexity, longer training/inference time, and a greater risk of overfitting to a single benchmark dataset if not validated with rigorous cross-validation and external test sets.

IX. COMPARATIVE ANALYSIS

Table consolidates representative quantitative results drawn from the reviewed literature. direct comparison should account for differing datasets, class counts, and validation protocols (single split vs. k-fold cross-validation).

Table 9. Representative transfer-learning CNN architectures used for brain tumour classification and reported accuracy ranges compiled from recent studies.

Method Family	Representative Technique	Reported Accuracy	Dataset	Relative Complexity
Classical ML	DWT + PCA + SVM (RBF)	~99%	Custom / Figshare-derived (binary)	Low
Classical ML	GLCM + SVM	98.9%	MRI (benign/malignant)	Low
Classical ML	Wavelet Energy + KNN	92–96%	Various small sets	Low
Ensemble Classical	KNN + Random Forest + Decision Tree (voting)	High (dataset-dependent)	Custom MRI set	Low–Medium
CNN (custom, shallow)	Lightweight custom CNN	98.1% – 99.6%	Br35H, Kaggle Brain Tumour MRI	Low–Medium
Transfer Learning	VGG16 (fine-tuned)	98.69% – 99.08%	Figshare, Kaggle	Medium
Transfer Learning	ResNet50 (fine-tuned)	96.67% – 99.15%	Figshare, Kaggle	Medium–High
Transfer Learning	EfficientNet family	Top-tier (often best overall)	Figshare, Kaggle	Medium

www.ijircce.com | e-ISSN: 2320-9801, p-ISSN: 2320-9798| Impact Factor: 9.927| ESTD Year: 2013|

International Journal of Innovative Research in Computer and Communication Engineering (IJIRCCE)

(A Monthly, Peer Reviewed, Refereed, Scholarly Indexed, Open Access Journal)

Method Family	Representative Technique	Reported Accuracy	Dataset	Relative Complexity
Transfer Learning	MobileNet / MobileNetV2	97.25% – 99.14%	Figshare, Kaggle	Low (efficient)
Transfer Learning	Xception	98.75% (F1)	Figshare	Medium–High
Attention / Hybrid CNN-Transformer	Attention-guided residual CNN / ResViT / UNetFormer	Competitive to SOTA	BraTS-derived, Kaggle	High
Hybrid (GAN + CNN + XAI)	GAN augmentation + ResNet50 + LIME	99.53%	Similar Kaggle-type dataset	High

9.1 Accuracy vs. Computational Cost

A consistent pattern across the reviewed studies is a trade-off between accuracy, interpretability, and computational cost rather than a single dominant method. Classical ML pipelines (GLCM/DWT + SVM/KNN) remain attractive where training data or compute is limited, offering fast training and reasonable accuracy on binary tasks, but they generally lag behind deep learning on multi-class problems and require careful, dataset-specific feature engineering. Lightweight CNNs (custom shallow networks, MobileNet) offer a strong accuracy-to-efficiency ratio suited to deployment on resource-constrained or mobile/edge devices. Deeper transfer-learning backbones (ResNet, EfficientNet, Xception) tend to achieve the highest accuracies on larger, more heterogeneous datasets (e.g., the aggregated Kaggle dataset) but at higher memory and inference cost. Attention-based and hybrid CNN-Transformer models achieve state-of-the-art or near-state-of-the-art results and add interpretability value through attention maps, at the highest computational cost and with typically greater data requirements.

X. CONCLUSION

From manually constructed texture-based pipelines with GLCM, DWT, and PCA using traditional classifiers (SVM, KNN) to neural networks based on deep transfer-learning CNNs (VGG/ResNet/EfficientNet/MobileNet) and attention-based/hybrid CNN-Transformer architectures for the final traces of research, brain tumour classification has advanced. For small-data binary tasks, classical machine learning (ML) is still competitive; transfer-learning CNNs provide the best-validated compromise between model performance and generalizability for multi-class MRI classification; attention and transformer-based hybrids currently define state of the art, but at a higher complexity cost; each generation makes different trade-offs in accuracy, interpretability, data scaling, and computation cost. This review's comparative evidence demonstrates that there is no universal winner. Future developments will rely more on addressing problems with data insufficiency, generalizability across institutions, and clinically actionable interpretability than on further architecture scaling.

REFERENCES

[1]. Chen, Y., Giudici, P., Kolesnikov, V., & Recchia, P. (2026). SAFE Quantum Machine Learning with Variational Quantum Classifiers. arXiv (Cornell University). https://doi.org/10.48550/arxiv.2605.16067.

[2]. Veneri, P. (2026). Interpretable four-class brain tumor MRI classification using a fine-tuned ResNet50. PeerJ Comput. Sci., 12, e3643.

[3]. Kurniawan, M. B., & Utami, E. (2025). Performance comparison of ReSNEt50, VGG16, and MobileNetV2 for brain tumor classification on MRI images. SISTEMASI, 14(2), 767. https://doi.org/10.32520/stmsi.v14i2.5054.

[4]. Rasheed M, Iqbal S, Jaffar A, Akram S. Advanced deep learning-based brain tumor classification using a novel customized CNN and optimized residual network. PLoS One. 2025 Oct 10;20(10):e0334430. doi: 10.1371/journal.pone.0334430.

[5]. Shahin, A. Fine-tuned ResNet34 for efficient brain tumor classification. Sci Rep **15**, 36910 (2025). https://doi.org/10.1038/s41598-025-20872-3

[6]. Bouhafra, S. et al. (2025). Deep Learning Approaches for Brain Tumour Detection and Classification Using MRI Images (2020 to 2024): A Systematic Review. Journal of Imaging Informatics in Medicine, 38(3), 1403-1433.

[7]. Deep Learning for Brain Tumour Segmentation and Classification: A Systematic Review of Methods and Trends (2025). ScienceDirect.

© 2026 IJIRCCE | Volume 14, Issue 7, July 2026 DOI: 10.15680/IJIRCCE.2026.1407071

www.ijircce.com | e-ISSN: 2320-9801, p-ISSN: 2320-9798| Impact Factor: 9.927| ESTD Year: 2013|

International Journal of Innovative Research in Computer and Communication Engineering (IJIRCCE)

(A Monthly, Peer Reviewed, Refereed, Scholarly Indexed, Open Access Journal)

[8]. Kumar, P.R., Prakash, K., Teja, B.R.S. et al. A novel brain MRI classification framework integrating tuned single scale retinex and empirical wavelet entropy features. Sci Rep **15**, 29765 (2025). https://doi.org/10.1038/s41598-025-13281-z.
[9]. Khan, M. et al. (2022). Convolutional Neural Network Techniques for Brain Tumour Classification (from 2015 to 2022): Review, Challenges, and Future Perspectives.
[10]. Sarah P, Krishnapriya S, Saladi S, Karuna Y and Bavirisetti DP (2024) A novel approach to brain tumor detection using K-Means++, SGLDM, ResNet50, and synthetic data augmentation. Front. Physiol. 15:1342572. doi: 10.3389/fphys.2024.1342572.
[11]. Reyes, D., & Sánchez, J. (2024). Performance of convolutional neural networks for the classification of brain tumors using magnetic resonance imaging. Heliyon, 10(3), e25468. https://doi.org/10.1016/j.heliyon.2024.e25468.
[12]. Rustom, F., Moroze, E., Parva, P., Ogmen, H., & Yazdanbakhsh, A. (2024). Deep learning and transfer learning for brain tumour detection and classification. Biology Methods and Protocols, 9(1), bpae080.
[13]. Khan, M. A., & Auvee, R. B. Z. (2024). Comparative Analysis of Resource-Efficient CNN Architectures for brain tumor Classification. arXiv (Cornell University). https://doi.org/10.48550/arxiv.2411.15596.
[14]. Dheepak, G., J, A. C., & Vaishali, D. (2024). Brain tumor classification: a novel approach integrating GLCM, LBP and composite features. Frontiers in Oncology, 13, 1248452. https://doi.org/10.3389/fonc.2023.1248452.
[15]. Subba, A. B., & Sunaniya, A. K. (2024). Computationally optimized brain tumor classification using attention based GoogLeNet-style CNN. Expert Systems With Applications, 260, 125443. https://doi.org/10.1016/j.eswa.2024.125443.
[16]. Abdusalomov, A. B. et al. (2024). Brain tumour detection based on deep learning approaches and magnetic resonance imaging. Cancers, 16(1), 1-19.
[17]. Brain Tumour Classification using VGG16, ResNet50, and Inception V3 Transfer Learning Models (2023).
[18]. Babu Vimala, B., Srinivasan, S., Mathivanan, S.K. et al. Detection and classification of brain tumor using hybrid deep learning models. Sci Rep **13**, 23029 (2023). https://doi.org/10.1038/s41598-023-50505-6.
[19]. Alemu, B. S., Feisso, S., Mohammed, E. A., & Salau, A. O. (2023). Magnetic resonance imaging-based brain tumor image classification performance enhancement. Scientific African, 22, e01963. https://doi.org/10.1016/j.sciaf.2023.e01963.
[20]. Kumar, A., Pandey, S.K., varshney, N. et al. Distinctive approach in brain tumor detection and feature extraction using biologically inspired DWT method and SVM. Sci Rep **13**, 22735 (2023). https://doi.org/10.1038/s41598-023-50073-9.
[21]. Sudeep, K. et al. (2022). Brain Tumour Classification using a Support Vector Machine. International Journal of Computer Applications, 184(28).
[22]. Maqsood, S., Damaševičius, R., & Maskeliūnas, R. (2022). Multi-modal brain tumour detection using deep neural network and multiclass SVM. Medicina, 58(8), 1090.
[23]. Garg, G., & Garg, R. (2021). Brain Tumor Detection and Classification based on Hybrid Ensemble Classifier. arXiv (Cornell University). https://doi.org/10.48550/arxiv.2101.00216.
[24]. Khan, H. A. et al. (2020). Brain tumour classification in MRI image using convolutional neural network. Mathematical Biosciences and Engineering, 17(5), 6203-6216.
[25]. Çinar, A., & Yildirim, M. (2020). Detection of tumours on brain MRI images using the hybrid convolutional neural network architecture. Medical Hypotheses, 139, 109684.
[26]. A Novel Method for Classifying Liver and Brain Tumours Using Convolutional Neural Networks, Discrete Wavelet Transform and Long Short-Term Memory Networks (2019).
[27]. Sultan, H. H., Salem, N. M., & Al-Atabany, W. (2019). Multi-classification of brain tumour images using deep neural network. IEEE Access, 7, 69215-69225.